Organic Electronics 14 (2013) 1197–1203

Contents lists available at SciVerse ScienceDirect

Organic Electronics

journal homepage: www.elsevier.com/locate/orgel

N-channel organic thin-film transistors based on a soluble cyclized perylene tetracarboxylic diimide dimer

Nianshuai An [a,1], Yanan Shi [a,1], Junqian Feng [b], Dapan Li [a], Jian Gao [a], Yanli Chen [a,*], Xiyou Li [b,*]

[a] Shandong Provincial Key Laboratory of Fluorine Chemistry and Chemical Materials, School of Chemistry and Chemical Engineering, University of Jinan, Jinan 250022, China
[b] Department of Chemistry, Shandong University, Jinan 250100, China

ARTICLE INFO

Article history:
Received 15 December 2012
Received in revised form 2 February 2013
Accepted 13 February 2013
Available online 27 February 2013

Keywords:
Perylenetetracarboxyl diimide
Dimer
Solution processing
N-channel semiconductor
Organic thin-film transistor

ABSTRACT

A high soluble dimeric perylene tetracarboxylic diimide (**1**) was fabricated into the thin solid films by means of *quasi-Langmuir–Shäfer* (QLS) method. The structure and properties of the QLS films were comparatively studied with those of monomeric perylene tetracarboxylic diimide (**2**) by electronic absorption, fluorescence, polarized electronic absorption spectroscopy, X-ray diffraction (XRD) and atomic force microscopy (AFM). Experimental results revealed the film crystallinity and general molecular order in the film of **1** are improved effectively in comparison with those of **2** due to the dimeric structure of **1**. Electron mobilities as high as 0.03 $cm^2 V^{-1} s^{-1}$ for the films of novel dimeric **1** are achieved, which is much better than that of monomeric **2** (5.0×10^{-7} $cm^2 V^{-1} s^{-1}$). In particular, the electronic mobility of **1** only slightly decreased after exposure to air and remained almost unchanged after 90 days, which is attributed to molecular packing effects including close stacking of dimeric PDI units and segregation effects imparted by the 2-N,N-di(n-butyl) amino-4,6-dihydrazine-1,3,5-trazine unites as well as relatively low-lying LUMO energy level. The present result represents not only the first example of solution-processed, air-stable dimeric PDI-based n-type OFET, but more importantly provides an efficient way to enhance the performance of air-stable *n*-channel organic semiconductors through intramolecular bonding to pre-organizing the π-conjugated organic molecules into a rigid cofacially stacked structure.

1. Introduction

Organic field-effect transistors (OFETs) with solution-processable organic semiconductors as active layers have attracted a significant research interest due to their potential applications in low-cost integrated circuits and flexible electronics [1–3]. Great progress has been achieved in the past decade towards developing novel semiconductor materials, especially those possessing π-conjugated electronic structure with high carrier mobility and good solubility in common organic solvents, such as conjugated polymers, oligomers of thiophenes, perylenes and phthalocyanines [4–8]. In addition to the intrinsic molecular chemical-physical properties and electronic structures of organic compounds, the performance of OFETs has been found to be closely related with the packing model of organic molecules in the solid state [9–11]. It has generally been accepted that maximizing π-orbital overlap between neighboring conjugated molecules is one good way to construct organic semiconductor thin films to reach high carrier mobility [12–16]. Various methods have been developed to enhance face-to-face stacking of conjugated semiconductor molecules in solid state by introducing different functional groups which are able to drive the assembly process to the prerequisite stacking. For instance, substituents were incorporated to pentacene molecules

* Corresponding authors. Tel.: +86 053189736150.
E-mail address: chm_chenyl@ujn.edu.cn (Y. Chen).
[1] These authors contributed equally to this work.

1566-1199/$ - see front matter © 2013 Elsevier B.V. All rights reserved.
http://dx.doi.org/10.1016/j.orgel.2013.02.012

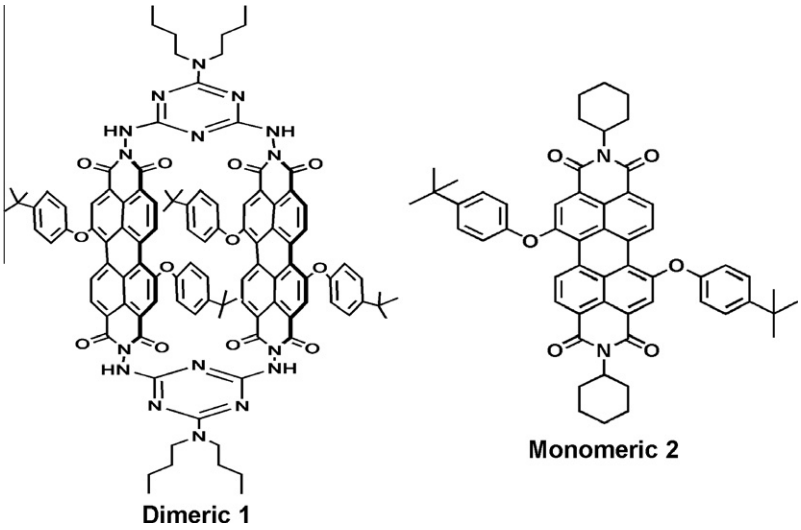

Fig. 1. Schematic structures of dimeric **1** and monomeric **2.**

to prevent C–H···π forces and induce more effective π–π interactions between pentacence molecules, thus leading to improved OFET properties [17–19]. Introduction of long alkoxy groups onto aromatic semiconductor molecules was also found to be helpful in improving the OFET properties as the liquid crystal property borrowed beneficial in promoting the π–π stacking and form ordered structure [20,21]. Using solution processing to modify molecular packing, the π–π stacking distance of 6,13-bis(triisopropylsilylethynyl) pentacene (TIPS-pentacene) was decreased from 3.33 Å to 3.08 Å, the hole mobility in TIPS-pentacene transistors increased from 0.8 $cm^2 V^{-1} s^{-1}$ to a high mobility of 4.6 $cm^2 V^{-1} s^{-1}$ [22]. Compared with highly developed *p*-channel organic semiconductors, n-type counterparts lag far behind for some major challenges such as: low mobility, poor stability in air, poor solubility for solution process, and large barriers to electron injection [23–25]. In organic electronics, *n*-type semiconductors are indispensable for the construction of diodes and complementary circuits with high operation speed and low power consumption. Perylene tetracarboxyl diimides (PDIs), a category of organic dyes with excellent thermal and photostability, have recently been intensively studied as good *n*-type semiconductors due to the high electron affinity caused by the electron-withdrawing imide groups [1,26–28]. Different functional groups have been introduced at the imide nitrogen atoms of PDIs with the aim of modifying the packing in solid state and thus improving the OFETs performance. Only a small amount of literature has addressed high performance PDI-based *n*-type organic semiconducting materials with good solution processability and device environmental stability [3]. As part of our continuous efforts towards the fabrication of ordered PDI-based nano-structures with potential application in OFET devices [7,29–33], in the present paper, a novel perylene tetracarboxylic diimide (PDI) dimeric molecule with four phenoxy groups at the 1,7-positions of the two PDI rings connected by two 2,4-diamino-1,3,5-triazine rings (**1**), Fig. 1, was employed in our study. The reasons we choose this compound are: (i) the two PDI rings covalently connected by two triazine spacers to form a cyclic rigid molecule, make the torsion of the PDI π system very small and favor a very dense molecular π–π stacking; and (ii) the phenoxy groups attached to two PDI units can improve its solubility in conventional organic solvents without disrupting the π-conjugation of the backbone [33], while the hydrophobic alkyl chains attached to two triazine rings provide sufficient flexibility for the optimization of noncovalent stacking of the perylene diimide π-systems. For comparative studies its monomeric counterpart (**2**) was also prepared. The devices with the *quasi-Langmuir–Shäfer* (QLS) films of the dimeric **1** as an active layer achieve a good *n*-type OFETs performance with the carrier mobility as high as 0.03 $cm^2 V^{-1} s^{-1}$ and on/off current ratio greater than 10^3, which is much better than that of the QLS films fabricated from the corresponding PDI monomer. To the best of our knowledge, this represents the first experimental effort towards constructing the structure–property correlations for the face-to-face stacked PDI dimer-based *n*-type semiconductor.

2. Experimental section

2.1. Chemicals

Dimer **1** and monomer **2** were synthesized according to previously published procedure [33]. Hexamethyldisilazane (HMDS) was purchased from Aldrich. All other reagents and solvents were of reagent grade and used as received.

2.2. Characterization

UV–vis spectra and polarized UV–vis spectra were recorded on a Hitachi U-4100 spectrophotometer. For the polarized absorption spectra recording, a dichroic sheet polarizer was placed in front of the QLS films with *s*- and *p*-polarized light, respectively. X-ray diffraction experiment was carried out on a Bruker AXS D8 ADVANCE X-

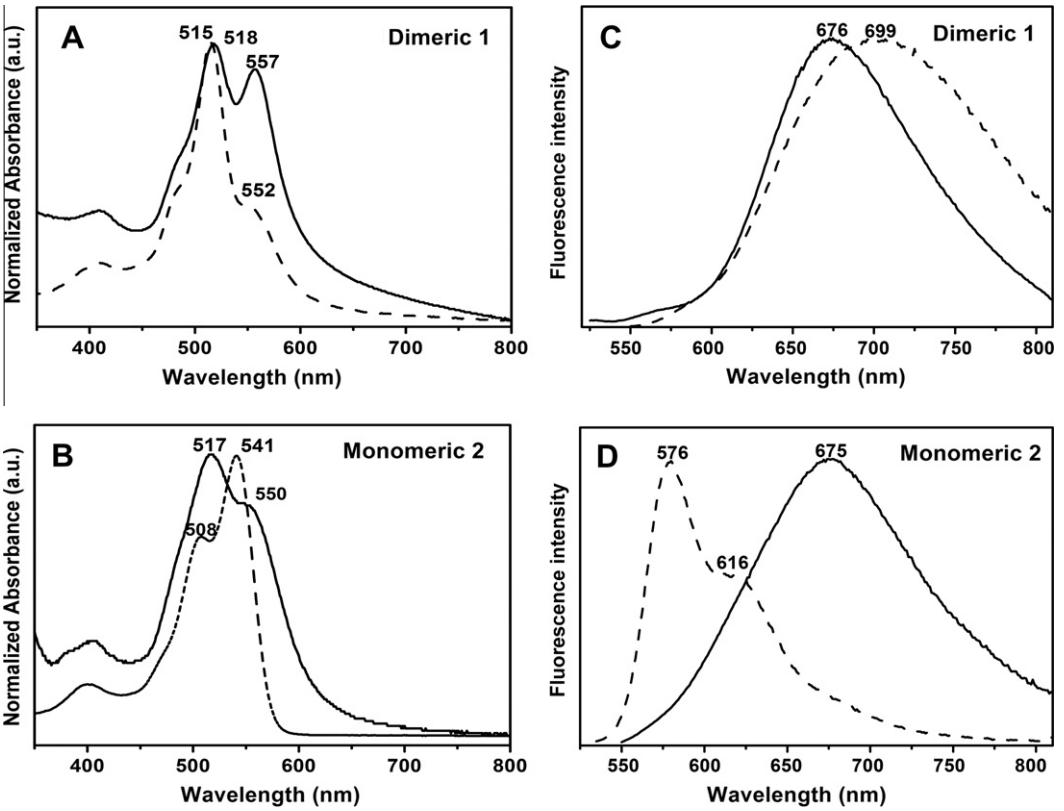

Fig. 2. Normalized electronic absorption (left) and fluorescence emission (right) spectra of dimer **1** (A and C) and monomer **2** (B and D) in CH_2Cl_2(dash line) and QLS films (solid line). The excited wavelength was 515 nm.

Table 1
The orientation angles of the PDI ring of **1** and **2** in the QLS films.

	$A_{//}$	$A_{\perp}$	$D_{0°}(A_{//}/A_{\perp})$	$A_{//}$	$A_{\perp}$	$D_{45°}$ ($A_{//}$ $A_{\perp}$)	θ (°)
Dimeric **1** (518 nm)	0.204	0.198	1.03	0.218	0.234	0.932	61.5
Monomeric **2** (516 nm)	0.284	0.243	1.17	0.263	0.276	0.953	67.1

ray diffractometer. AFM images were collected in air under ambient conditions using the tapping mode with a NanoscopeIII/Bioscope scanning probe microscope from Digital instruments.

2.3. OTFT device fabrication

Before depositing the QLS films of dimeric **1** and monomeric **2**, surface treatment for SiO_2/Si substrates was performed according to literature method using HMDS [34]. OTFT devices were fabricated on a HMDS-treated Si/SiO_2 (300 nm thickness, capacitance $C_0 = 10$ nF cm^{-2}) substrate by evaporating gold electrodes onto the QLS films of **1**–**2** employing a shadow mask. Electrodes with two sets of dimensions ($W = 8.16$ mm, $L = 145$ μ m, $W/L = 56$ and $W = 28.6$ mm, $L = 240$ μm, $W/L = 119$) were used for OFET measurements. The drain-source current (I_{ds}) versus drain-source voltage (V_{ds}) characteristic was obtained with a Hewlett-Packard (HP) 4140B parameter analyzer at room temperature. QLS films were prepared following the method published previously [35]. In the present case, the 10-layer QLS films of **1**–**2** were obtained for OFET measurements.

3. Resulted and discussion

3.1. Electronic absorption and fluorescence emission spectra

The electronic absorption and emission spectra of compounds dimer **1** and monomer **2** in $CHCl_3$ and the QLS films were recorded and shown in Fig. 2. The absorption spectrum of dimer **1** in solution has a characteristic vibronic structure associated with the π–π electronic transitions of PDI chromophores with a 0–1 band at 515 nm and 0–0 band at 552 nm. This absorption spectrum corresponds well to many other folded and circular perylene dimers reported previously [7,33,36]. The intensity of the vibrational transitions within the progression follows the order 0–1 > 0–0, which is commonly attributed to the intramolecular π–π stacking in PDI dimer in solution [33,36].

Furthermore, the main absorption band for dimer **1** in solution is blue-shifted with respect to that of monomer **2**. This observation confirms the face-to-face stacked molecular geometry between the two PDI rings in the dimeric compound [7,33,37,38]. The absorption spectra of dimer **1** in QLS films, Fig. 2A, show no significant shift in the main absorption band in comparison with that in solution. This indicates that the face-to-face dimeric structure is well preserved in the QLS films. A new peak at 557 nm derived from π–π interactions of the chromophores in the solid state appeared, indicating that a crystalline thin film was formed by overlapping neighboring perylene moieties of dimer **1** [39,40]. By comparing the absorption spectrum of 2 in solution, the relative enhancement of the 0–1 transition in the QLS film of **2** was shown by the normalized absorption spectra, Fig. 2B, which implied the formation of H-type (face-to-face) aggregation [21,41,42]. Consistent with the absorption measurement, the fluorescence spectra in the QLS films showed a new emission at about 702 nm for **1** and 675 nm for **2**, respectively (Fig. 2C and D), which is a typical emission of PDI excimer-like state, suggesting strong π–π stacking and a typical H-type (face-to-face) aggregation configuration [30,43,44]. More interestingly, emission maxima appeared in the QLS films of **2** (ca. 675 nm) is almost the same position as that of **1** in solution (ca. 676 nm). This not only further validates the face-to-face stacked molecular geometry between the two PDI rings of **1** but also indicates the co-facial dimer formation in the QLS films of **2**. The effective intermolecular face-to-face interaction in the H aggregates together with the intense intramolecular π–π stacking in dimer **1** provide the π electrons with an extensive area for delocalization. This forms the most basic necessary characteristics for an organic semiconductor with good charge transport ability [45].

3.2. Orientation of PDI ring in the QLS films

Further information on the molecular organization in the QLS films of these compounds was obtained by polarized UV–vis spectroscopic technique. The polarized UV–vis spectra of QLS films on glass substrate were recorded with an incidence angle of 0° and 45°, respectively, Fig. S1 (Supplementary material), and the data are summarized in Table 1. The orientation angles of PDI ring can be calculated by the method of Yoneyama et al. [46]. The tilt angles of the PDI rings of **1** and **2** were calculated to be 61.5° and 67.1° respectively, which are larger than the magic angle 54.7°. A slipped co-facial stacking mode (H-aggregate) was achieved for either **1** or **2** in the QLS films according to the exciton theory [36], which is consistent with their aggregation behaviors deduced from electronic absorption and emission spectra.

3.3. X-ray diffraction patterns

For most of the applications, the properties of the devices are closely related to the structure of solid films [10,11,35,47]. The quality of the thin solid films can be assessed using X-ray diffraction technique, which is helpful for understanding the microstructure–function relationship between molecular ordering in organic thin films and charge transport properties [26]. As shown in Fig. 3A, in the low-angle range, the XRD diagram of QLS films of **1** deposited on glass substrate shows three well-defined diffraction peaks at $2\theta = 2.88°$, 5.74° and 8.24°, which are ascribed to the diffractions from the (001), (002) and (003) planes, respectively. This implies that QLS films of **1** had an long-range order across its thickness [10,35,48]. The *d* spaces calculated according to the Bragg equation is about 3.07 nm and corresponding to the distance between two adjacent PDI **1** molecules in the longitudinal direction. Judging from a geometry-optimized, molecular length (3.40 nm) of dimer **1** molecule, the tilt angle relative to the substrate of 64.5° is obtained. This corresponds well with the result of polarized UV–vis spectra, indicating again that dimer **1** molecules take a slipped co-facial stacking mode with an "edge-on" configuration in the QLS films. In addition, a broad peak at 0.42 nm for the dimer **1** films suggested that there exists liquid-like ordered packing of long alkyl chains [30,49]. A higher-order diffraction is found at 0.31 nm for dimer **1** films, which can be attributed to the formation of efficient π–π stacking with face-on orientations [29–32]. It is therefore expected that dimer **1** films would be able to adopt 3-D conduction channels that would decrease the barrier of charge transport over that of the QLS films with only perpendicular π–π planes [50], in turn contributes to the excellent electron mobility revealed

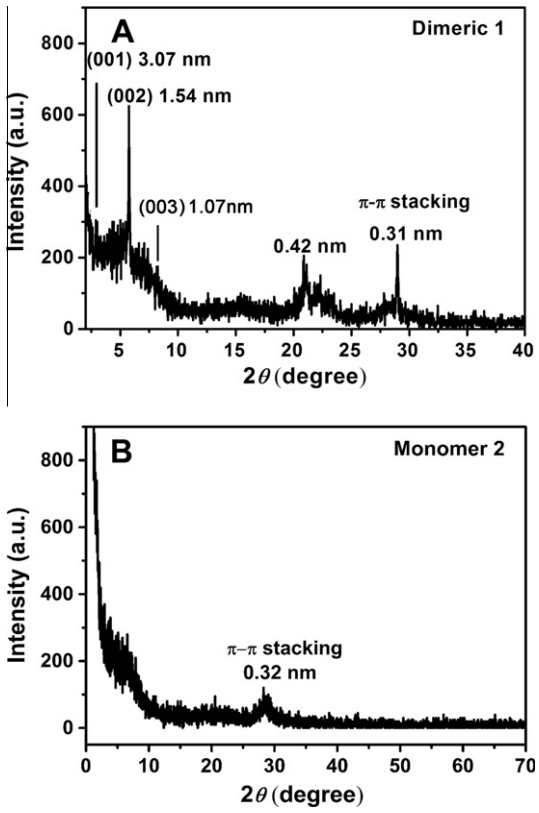

Fig. 3. X-ray diffraction patterns of compound dimer **1** (left) and monomer 2 (right) films on SiO_2/Si substrate.

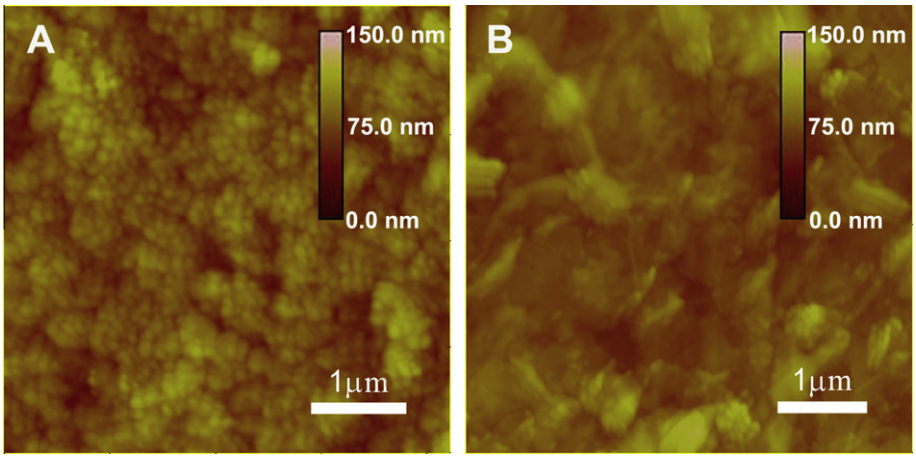

Fig. 4. AFM images of the QLS films of dimeric **1** (A) and monomeric **2** (B).

for the devices fabricated with **1** (*vide infra*). In the case of the films of **2**, only a weak π–π stacking feature at 0.32 nm is observed without the presence of a lamellar structure evidenced by the absence of any diffraction peaks in the low-angle range. The better crystallinity in the QLS films of **1** compared to that of **2** can be related to not only improved co-planarity by the unique co-facially dimeric structure, but more importantly the minimization of steric repulsions by the substituent alkyl side chains (which results in a highly ordered and denser molecular packing and aligned nature of dimeric 1 in the films). Obviously, the more closer π–π stacking and higher molecular order as well as increased crystallinity existed in the QLS films of **1** than those of **2**, which is expected to provide more efficient orbital overlap and thereby facilitates charge transport between source-to-drain electrodes [31,51].

3.4. AFM surface topography

AFM provides more information on the aspect of the QLS films and therefore allows us to correlate the morphology and electrical properties. Fig. 4 compares the morphologies of the QLS films of dimer **1** and monomer **2** deposited on the SiO_2/Si substrate. The surface of the QLS films of **1** exhibits a granular structure with the average diameter of ca. 100 nm,and root mean square (Rms) roughness value of 7.69, Fig. 4A, whereas that of **2** presents a larger grain size with a non-uniform morphology and a higher Rms value of 36.8, Fig. 4B. The more uniform grain size and much lower Rms value for the QLS films of **1** will significantly decrease gaps between the grains and crack formation in the film, and thus improving the carrier mobility [52].

3.5. OFET properties

To further determine the majority carrier type and corresponding mobility of these compounds, typical top-contact/bottom-gate configuration OFET devices, in which the source and drain electrodes are vacuum-deposited on the top of the QLS films of **1–2**, have been fabricated. OFET properties were evaluated under positive or negative gate bias in both air and N_2 to explore the majority charge carrier type, device performance, and environmental stability. Experimental data were analyzed using standard field-effect transistor equations:

$$I_{ds} = (W/2L)\mu C_0(V_g - V_{th})^2$$

where I_{ds} is the source-drain current, V_g is the gate voltage, C_0 is the capacitance per unit area of the dielectric layer, and V_{th} is the threshold voltage, and μ is the mobility in the saturation region [53]. The mobilities were determined in the saturation regime from the slope of plots of $(I_{ds})^{1/2}$ versus V_g. As shown in Fig. 5, the positive gate and source-drain voltages indicate that the QLS films of dimer **1** are of *n*-type characteristics in both air and N_2. Both devices show significant contact resistance, as evidenced from the nonlinearity of the output curve at low source-drain voltage, and can be attributed to the non-ideal semiconductor–metal interface [54]. Electron mobility of about 0.03 and 0.02 $cm^2\ V^{-1}\ s^{-1}$ for dimer **1** is observed in N_2 and air, respectively (with current on/off ratios on the order of $\sim 10^3$–10^4). In addition, over 90% devices of dimer **1** exhibited electron mobility over 0.02 $cm^2\ V^{-1}\ s^{-1}$ with the highest electron mobility near 0.1 $cm^2\ V^{-1}\ s^{-1}$ measured in the nitrogen glove-box. The electronic mobility of **1** only slightly decreased after exposure to air and remained stable for more than 90 days. It is worth noting that no *p*-channel behavior was observed in both air and N_2, similar to the OFET behaviors of the monomeric PDI-based molecules with no substituents at the bay positions (1,6,7,12 positions of the perylene core) reported previously [54]. As for monomer **2**, we observed both *p*- and *n*-channel transistor behavior with significantly lower hole and electron mobility, $\sim 6.0 \times 10^{-4}$ and $\sim 5.0 \times 10^{-7}$ measured in air and N_2, respectively, Fig. S2 (Supplementary material). As a consequence, enhanced electron transport performance was achieved just *via* increasing the number of PDI units within one PDI-based molecule for the first time. Note that compound **1** seems to represent also the first example of solution-processable *n*-type dimeric PDI-based semiconductor, to the best of our knowledge. Actually, OFET characteristics have been tested using electrodes

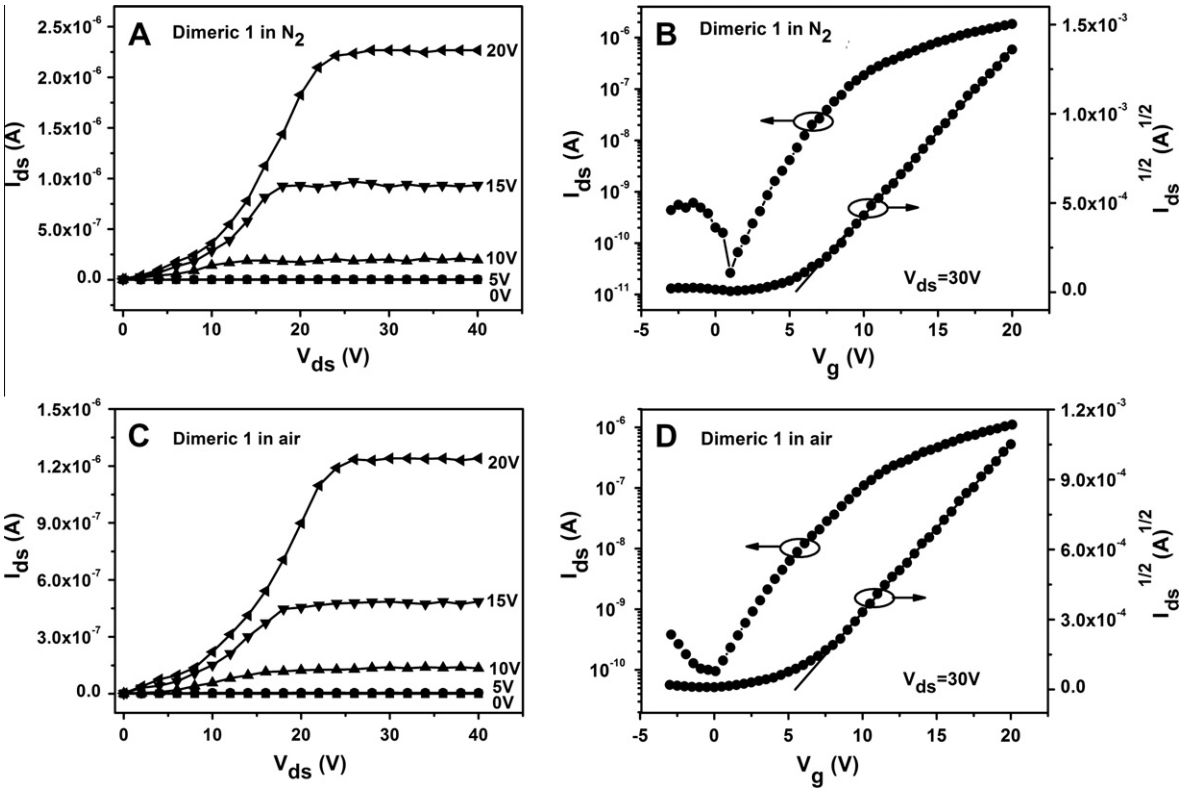

Fig. 5. Drain-source current (I_{ds}) versus Drain-source voltage (V_{ds}) characteristic at different gate voltage (left) and transfer curve (right) for dimeric **1** in air (A and B) and in N_2 (C and D), respectively, on the HMDS-treated SiO_2/Si substrates with the Au electrode at channel length L = 145 μm.

with two sets of dimensions (channel length at L = 145 and 240 μm with the W/L ratio of 56 and 119, respectively), no evidence was revealed for the effect of the geometric factors on the OFET mobilities in present case. However, all the devices based on **1** showed higher contact resistance (caused by the nonideal semiconductor–metal interface) at channel length L = 240 μm (Fig. S3, Supplementary material), while better interface contacts were founded for L = 145 μm (Fig. 5). This may be the result of the different thin-film quality between compound **1** and **2**. Table S1 summarizes the OFET parameters for compound **1**.

Investigations have revealed that the energy levels of the highest occupied molecular orbital (HOMO) and the lowest unoccupied molecular orbital (LUMO) are crucial in determining the majority charge carrier and charge carrier stability of organic semiconductors [55,56]. In the present case, the HOMO and LUMO energy levels of **1**–**2** can be estimated from their half-wave potentials of the first and second reductions (versus SCE) obtained by cyclic voltammetry [33]. As summarized in Table S2 (Supplementary material), both the HOMO and LUMO energy levels of −6.16 and −3.89 eV for dimer **1** are smaller than those of −5.88 and −3.77 eV for monomer **2**, indicating that dimer **1** are harder to be oxidized and easier to be reduced than monomer **2**. Therefore, the larger electron mobility of dimer **1** relative to that of monomer **2** is probably closely related to the lower LUMO energy levels enabled by the enhanced molecular packing, which results in the smaller injection barriers for electrons with regard to the gold contacts [57]. Normally, an air-stable n-type semiconductor needs a LUMO energy level lower than −4.0 eV to against the air-derived electron traps [26,58]. The LUMO energy level of **1** still does not meet this request. Obviously, monomer **2** does not satisfy this condition too which corresponds well with the fact that the n-type semiconductor properties of the monomer 2 can be detected only under an inert atmosphere [59]. The un-expected air stability of dimer **1** OFETs is thought to be strongly related with the molecular packing and morphology of the thin films [51,52]. The densely packed PDI cores together with the closely packed liquid-like ordered alkyl chains may provide a kinetic barrier to the diffusion of oxygen and moisture into the channel region. On the other hand, the energy-optimized conformation of **1** obtained from the DFT calculation (B3LYP/6-31G(d)) indicates that dimer **1** includes a rigid face-to-face configuration with a inter-planar distance of 4.8 nm, while the in-plane torsion angle between the long axis of the two PDI rings and the dihedral between the PDI planes are close to zero [33]. Such molecular structural characteristics are expected conventionally to reduce the reorganization energy of PDI molecules with a greater magnitude, which should be highly responsible for the higher electron mobility of dimer **1** than that of monomer **2** [60]. Additionally, the superior charge transport performance of the dimeric **1** TFTs might also be related to stronger intermolecular interactions in the QLS films through the incorporation of flexible alkyl -solubilizing chains to a rigid co-facially stacked structure. This

conclusion is consistent with the results of the XRD and morphological analyses.

4. Conclusions

We have presented good *n*-channel OFET properties of the QLS films of a novel PDI dimer **1,** with a carrier mobility as high as 0.03 $cm^2 V^{-1} s^{-1}$. Very dense and rigid face-to-face arrangement of undistorted PDI planes as well as the good film crystallinity facilitate charge carrier transport. In particular, the thin-film OFETs of PDI dimer **1** exhibit long-term air-stable operation, despite the absence of electron-withdrawing substituent at the aromatic core. The results suggested that molecular packing effects including densely packed PDI cores together with the closely packed liquid-like ordered alkyl chains are crucial for air stability. This provides an efficient way to enhance the performance of air-stable *n*-channel organic semiconductors through intra-molecular bonding to pre-organizing the π-conjugated organic molecules into a rigid co-facially stacked structure.

Acknowledgements

The authors would like to thank the Natural Science Foundation of China (20871055, 21073112) and the Natural Science Foundation of Shandong Province (ZR2011BZ005, ZR2010EZ007) for the financial support of this work.

Appendix A. Supplementary material

Supplementary data associated with this article can be found, in the online version, at http://dx.doi.org/10.1016/j.orgel.2013.02.012.

References

[1] C.D. Dimitrakopoulos, P.R.L. Malenfant, Adv. Mater. 14 (2002) 99.
[2] R. Li, W. Hu, Y. Liu, D. Zhu, Acc. Chem. Res. 43 (2010) 29.
[3] H. Usta, A. Facchetti, T.J. Marks, Acc. Chem. Res. 44 (2011) 501.
[4] W. Wu, Y. Liu, D. Zhu, Chem. Soc. Rev. 39 (2010) 1489.
[5] R.P. Ortiz, A. Facchetti, T.J. Marks, Chem. Rev. 110 (2010) 205.
[6] S. Liu, W.M. Wang, A.L. Briseno, S.C.B. Mannsfeld, Z. Bao, Adv. Mater. 21 (2009) 1217.
[7] Y. Wang, Y. Chen, R. Li, S. Wang, X. Li, J. Jiang, Langmuir 23 (2007) 5836.
[8] J. Kan, Y. Chen, D. Qi, Y. Liu, J. Jiang, Adv. Mater. 24 (2012) 1755.
[9] K. Xiao, Y. Liu, G. Yu, D. Zhu, Appl. Phys. A 77 (2003) 367.
[10] Y. Chen, D. Li, N. Yuan, J. Gao, R. Gu, G. Lu, M. Bouvet, J. Mater. Chem. 22 (2012) 22142.
[11] Y. Chen, W. Su, M. Bai, J. Jiang, X. Li, Y. Liu, L. Wang, S. Wang, J. Am. Chem. Soc. 127 (2005) 15700.
[12] M. Bendikov, F. Wudl, D. Perepichka, Chem. Rev. 104 (2004) 4891.
[13] G.R. Hutchison, M.A. Ratner, T.J. Marks, J. Am. Chem. Soc. 127 (2005) 16866.
[14] M. Halik, H. Klauk, U. Zschieschang, G. Schmid, S. Ponomarenko, S. Kirchmeyer, W. Weber, Adv. Mater. 15 (2003) 917.
[15] A. Facchetti, M.H. Yoon, C.L. Stern, H.E. Katz, T.J. Marks, Angew Chem. Int. Ed. 42 (2003) 3900.
[16] Q. Miao, M. Lefenfeld, T.Q. Nguyen, T. Siegrist, C. Kloc, C. Nuckolls, Adv. Mater. 17 (2005) 407.
[17] J.E. Anthony, D.L. Eaton, S.R. Parkin, Org. Lett. 4 (2002) 15.
[18] J.E. Anthony, J.S. Brooks, D.L. Eaton, S.R. Parkin, J. Am. Chem. Soc. 123 (2001) 9482.
[19] H. Meng, M. Bendikov, G. Mitchell, R. Holgeson, F. Wudl, Z. Bao, T. Siegrist, C. Kloc, C.H. Chen, Adv. Mater. 15 (2003) 1090.
[20] C.D. Simpson, J. Wu, M.D. Watson, K. Müllen, J. Mater. Chem. 14 (2004) 494.
[21] Z. An, J. Yu, S.C. Jones, S. Barlow, S. Yoo, B. Domercq, P. Prins, L.D.A. Siebbeles, B. Kippelen, S.R. Marder, Adv. Mater. 17 (2005) 2580.
[22] G. Giri, E. Verploegen, S.C.B. Mannsfeld, S.A. Evrenk, D.H. Kim, S.Y. Lee, H.A. Becerril, A.A. Guzik, M.F. Toney, Z. Bao, Nature 480 (2011) 504.
[23] X. Mu, W. Song, Y. Zhang, K. Ye, H. Zhang, Y. Wang, Adv. Mater. 22 (2010) 4905.
[24] C.R. Newman, C.D. Frisbie, D.A. da Silva, J.L. Bredas, P.C. Ewbank, K.R. Mann, Chem. Mater. 16 (2004) 4436.
[25] J. Zaumseil, H. Sirringhaus, Chem. Rev. 107 (2007) 1296.
[26] B.A. Jones, A. Facchetti, M.R. Wasielewski, T.J. Marks, J. Am. Chem. Soc. 129 (2007) 15259.
[27] F. Würthner, Angew Chem. Int. Ed. 40 (2001) 1037.
[28] A. Kraft, Chem. Phys. Chem. 2 (2001) 163.
[29] L. Xue, H. Wu, Y. Shi, H. Liu, Y. Chen, X. Li, Soft Matter 7 (2011) 6213.
[30] H. Wu, L. Xue, Y. Shi, Y. Chen, X. Li, Langmuir 27 (2011) 3074.
[31] Y. Chen, Y. Kong, Y. Wang, P. Ma, M. Bao, X. Li, J. Colloid Interface Sci. 330 (2009) 421.
[32] Y. Chen, Y. Feng, J. Gao, M. Bouvet, J. Colloid Interface Sci. 368 (2012) 387.
[33] J. Feng, Y. Zhang, C. Zhao, R. Li, W. Xu, X. Li, J. Jiang, Chem. Eur. J. 14 (2008) 7000.
[34] H.Z. Chen, M.M. Ling, X. Mo, M.M. Shi, M. Wang, Z. Bao, Chem. Mater. 19 (2007) 816.
[35] Y. Chen, M. Bouvet, T. Sizun, Y. Gao, C. Plassard, E. Lesniewska, J. Jiang, Phys. Chem. Chem. Phys. 12 (2010) 12851.
[36] A.E. Clark, C. Qin, A.D.Q. Li, J. Am. Chem. Soc. 129 (2007) 7586.
[37] M. Kasha, H.R. Rawls, M.A. El-Bayoumi, Pure Appl. Chem. 11 (1965) 371.
[38] M.J. Ahren, L.E. Sinks, B. Rybtchinski, W. Liu, B.A. Jones, J.M. Giaimo, A. Gusev, A. Goshe, D.M. Tiede, M.R. Wasielewki, J. Am. Chem. Soc. 126 (2004) 8284.
[39] D. Schlettwein, H. Graaf, J.P. Meyer, T. Oekermann, N.I. Jaeger, J. Phys. Chem. B 103 (1999) 3078.
[40] J. Mizuguchi, J. Appl. Phys. 84 (1998) 4479.
[41] P.P. Neelakandan, Z. Pan, M. Hariharan, Y. Zheng, H. Weissman, B. Rybtchinski, F.D. Lewis, J. Am. Chem. Soc. 132 (2010) 15808.
[42] J.M. Giaimo, A.V. Gusev, M.R. Wasielewski, J. Am. Chem. Soc. 124 (2002) 8530.
[43] F. Würthner, Z. Chen, V. Dehm, V. Stepanenko, Chem. Commun. (2006) 1188.
[44] A. You, J. Gao, D. Li, M. Bouvet, Y. Chen, Supramol. Chem. 24 (2012) 851.
[45] H.E. Katz, Z. Bao, J. Phys. Chem. B 104 (2000) 671.
[46] M. Yoneyama, M. Sugi, M. Saito, K. Ikegami, S. Kuroda, S. Lizima, Jpn. J. Appl. Phys. 25 (1986) 961.
[47] J. Simon, P. Bassoul, Design of Molecular Materials: Supramolecular Engineering, John Wiley & Sons, London and New York, 2001.
[48] T.J. Prosa, M.J. Winokur, J. Moulton, P. Smith, A.J. Heeger, Macromolecules 25 (1992) 4364.
[49] F. Würthner, C. Thalacker, S. Diele, C. Tschierske, Chem. Eur. J. 7 (2001) 2245.
[50] J. Lee, A.-R. Han, J. Kim, Y. Kim, J.H. Oh, C. Yang, J. Am. Chem. Soc. 134 (2012) 20713.
[51] B.A. Jones, M.J. Ahrens, M.-H. Yoon, A. Facchetti, T.J. Marks, M.R. Wasielewski, Angew Chem. Int. Ed. 43 (2004) 6363.
[52] J.H. Oh, S. Liu, Z. Bao, R. Schmidt, F. Würthner, Appl. Phys. Lett. 91 (2007). 212107-1.
[53] S.M. Sze, In Physics of Semiconductor Devices, John Wiley & Sons, New York, 1981.
[54] A.L. Briseno, S.C.B. Mannsfeld, C. Reese, J.M. Hancock, Y. Xiong, S.A. Jenekhe, Z. Bao, Y. Xia, Nano Lett. 7 (2007) 2847.
[55] A. Facchetti, M. Mushrush, H.E. Katz, T.J. Marks, Angew Chem. Int. Ed. 15 (2003) 33.
[56] P. Ma, J. Kan, Y. Zhang, C. Hang, Y. Bian, Y. Chen, N. Kobayshi, J. Jiang, J. Mater. Chem. 21 (2011) 18552.
[57] G. Giri, E. Verploegen, S.C.B. Mannsfeld, S. Atahan-Evrenk, D.H. Kim, S.Y. Lee, H.A. Becerril, A. Aspuru-Guzik, M.F. Toney, Z. Bao, Nature 480 (2011) 504.
[58] Z. Wang, C. Kim, A. Facchetti, T.J. Marks, J. Am. Chem. Soc. 129 (2007) 13362.
[59] R. Schmidt, J.H. Oh, .Y.S. Sun, M. Deppisch, A.M. Krause, K. Radacki, H. Braunschweig, M. Könemann, P. Erk, Z. Bao, F. Würthner, J. Am. Chem. Soc. 131 (2009) 6215.
[60] Y.C. Chang, I. Chao, J. Phys. Chem. Lett. 1 (2010) 116.